

SPACE RESEARCH COORDINATION CENTER



**AN INTERFEROMETRIC STUDY OF DISSOCIATIVE
RECOMBINATION RADIATION IN NEON
AND ARGON AFTERGLOWS**

BY

**LOTHAR FROMMHOLD AND MANFRED A. BIONDI
DEPARTMENT OF PHYSICS**

SRCC REPORT NO. 92

**UNIVERSITY OF PITTSBURGH
PITTSBURGH, PENNSYLVANIA**

10 FEBRUARY 1969

An Interferometric Study of Dissociative Recombination Radiation
in Neon and Argon Afterglows*

Lothar Frommhold** and Manfred A. Biondi

Physics Department

University of Pittsburgh

Pittsburgh, Pennsylvania

January 1969

*This research was supported, in part, by the U. S. Office of Naval Research, Nonr - 624-(13).

**Present address, Physics Department and Electronics Research Center, University of Texas, Austin, Texas.

An Interferometric Study of Dissociative Recombination Radiation
in Neon and Argon Afterglows*

Lothar Frommhold** and Manfred A. Biondi
 Physics Department, University of Pittsburgh, Pittsburgh, Pennsylvania

Abstract

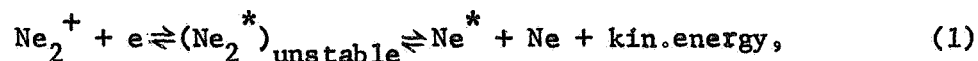
A photoelectric recording, pressure tuned Fabry-Perot interferometer of high resolution is used to determine the spectral line profiles of 22 neon and 5 argon ($2p_n \rightarrow 1s_m$) lines emitted from a microwave discharge and during the ensuing afterglow. All afterglow line profiles are broader than the corresponding discharge lines, and in most cases the afterglow line shapes are consistent with a dissociative origin of the excited atoms, indicating that the $2p_n$ excited states of neon and argon are produced by dissociative recombination of electrons with Ne_2^+ and Ar_2^+ ions, respectively. Detailed examination of the line profiles in neon indicates a "multi-shouldered" structure corresponding to several different dissociation kinetic energies, suggesting that different initial states of the Ne_2^+ ion are involved in the dissociative recombination process. From the deduced molecular ion energy levels it appears that, in addition to the Ne_2^+ ion state with a dissociation energy $D = 1.35$ eV reported by Connor and Biondi, there may be a more weakly bound state with $D \sim 0.5$ eV which contributes to the recombination.

*This research was supported, in part, by the U. S. Office of Naval Research, Nonr - 624(13).

**Present address, Physics Department and Electronics Research Center, University of Texas, Austin, Texas.

I. Introduction

In an earlier study⁽¹⁾, the capture rate of electrons by ions in neon was shown to result from the dissociative recombination process, i.e.



where the superscripts + and * indicate ionized and excited states, respectively. These afterglow studies made use of an interferometer to detect kinetic energy of the excited atoms produced by the dissociative process (through the corresponding Doppler effect on the emitted line profiles).

The studies⁽¹⁾ showed that the $\lambda 5852$ ($2p_1 \rightarrow 1s_2$) afterglow recombination radiation evidently consisted of a thermal doppler core sitting atop a trapezoidal dissociative pedestal. The dissociative (trapezoidal) portion of the line profile has been shown⁽²⁾ to be given by

$$I(\tilde{\nu}) = (a/4b) [\text{erf}(\tilde{\nu} + b) - \text{erf}(\tilde{\nu} - b)], \quad (2)$$

where $a = (Mc^2/kT)^{1/2} / \tilde{\nu}$ and $b = (E_D/kT)^{1/2}$; $\tilde{\nu}$ and $\tilde{\nu}_0$ are the frequencies (in wave numbers), the subscript 0 referring to the line center, M is the mass of the atom in the diatomic ion, E_D is the dissociation kinetic energy and T is the ions' kinetic temperature. Such a profile would arise if a single dissociation energy E_D (see curves i_2 and x_2 in Fig. 1) alone is involved. This in turn, implies that only one stable molecular ion curve and one repulsive excited molecule curve contribute to the process and that the ions are all in the same vibrational state. Thus, the line profiles were interpreted as resulting from a fraction of fast, dissociatively produced excited atoms which radiated before losing their excitation (trapezoidal profile), with the thermal Doppler core arising from those fast atoms which had undergone excitation transfer

collisions with the ambient (ground state) atoms before radiation occurred.

In the present work, a substantial improvement in signal-to-noise ratio has been achieved, and many additional afterglow lines in neon and in argon have been studied. These studies have revealed dissociative broadening in all cases but have shown that the spectral line profiles are more complex than was assumed in the earlier analysis⁽¹⁾, which was based on a line profile arising from a single dissociation energy plus a thermal Doppler core. The present paper gives examples of the more accurately determined line profiles in neon and in argon afterglows and proceeds to analyze the details of the profiles to provide a more realistic picture of the energy states of the Ne_2^+ ion than was obtained in the earlier work.

II. Apparatus

A detailed description of the microwave afterglow and optical interferometer system was given earlier by Connor and Biondi⁽¹⁾. The Fabry-Perot interferometer consists of a 1"D. aperture, $\lambda/100$ flat set of plates with multilayer dielectric films of 95 - 97% reflectivity over the wavelength range studied. The overall instrumental finesse (considering plate flatness, film reflectivity and exit aperture size) exceeded ~ 30 for the optical transitions studied. Three modifications of the apparatus have been made for the present studies, which we briefly discuss here. In order to extend the former study to other afterglow lines of neon and argon, a monochromator is used following the interferometer instead of an interference filter (see Fig. 2). Its resolution is high enough that two lines having a wavelength difference of more than 14 \AA can be satisfactorily separated even if their intensity ratio is as disparate as 1:10. In this way, most of the strong $2p - 1s$ transitions⁽³⁾ in Ne and in Ar could be studied, totaling 22 such transitions in Ne and 5 in Ar. (In addition, some higher transitions such as $3s - 2p$ and $4d - 2p$ have been studied in Ne).

A crucial problem has been the intensity of the afterglow light, and

substantial efforts have been made toward improvement of the signal-to-noise ratio of the system. In the interferometer design, a small exit iris is used and thus only a small fraction of the detecting photomultiplier cathode is needed for signal detection. The remaining parts of the cathode contribute only to the dark current noise of the device; therefore, by magnetically defocusing most of the off-axis electrons in the linear, venetian blind photomultiplier tube^(4,5), in addition to dry ice cooling of the tube, (see Fig. 2) both the dark current and the associated noise per unit bandwidth have been reduced to $< 10^{-12}$ Amp. and the sensitivity maintained (200 Amp/lm). This corresponds to an increase in the signal-to-noise ratio of almost two orders of magnitude over the previous work⁽¹⁾, and the remaining noise in the recordings is almost entirely due to statistical fluctuations of the signal current itself (i.e., signal shot noise).

III. Structure of the Afterglow Line Profiles

In the dissociative recombination process, for a Ne_2^+ ion in the state given by the schematic potential curve i_1 in Fig. 1, the energy E_D' will be transformed along the curve x_1 into kinetic energy of the dissociating atoms $\text{Ne}^* + \text{Ne}$ (one of the atoms is left in a particular excited 2p level). If the excited atom radiates by a transition into a particular 1s state before either a momentum transfer or an excitation transfer collision takes place, then the shape of the spectral line emitted is of a trapezoidal form⁽²⁾, due to Doppler broadening. (Here we assume $E_D' \gtrsim 3 \text{ kT}$.) From Eq. (2), it can be shown that the rising or falling shoulders of the trapezoid's sides have a "frequency extent", in wave number units, taken from 15 to 85% of the central height, which is given by

$$R = 2\tilde{\nu}_0 (kT/Mc^2)^{1/2}. \quad (3)$$

The "frequency" half-width of the trapezoid is

$$H = 2\hat{v}_0 (E_D/Mc^2)^{1/2}. \quad (4)$$

Momentum transfer collisions (i.e. ordinary elastic collisions) would reduce the width of the trapezoid⁽¹⁾. In our present work the rate of elastic collisions has been kept small; thus, to a first approximation, their effect may be neglected.

There is an additional factor which may affect the lineshape of a given $2p_n - 1s_m$ transition: cascading. Suppose the excited Ne state produced in a dissociative recombination reaction is a higher lying state than $2p$ (say a $3s$ state). Then the energy E_D available for dissociative Doppler broadening would be smaller. Hence, a relatively narrow line might be noted in a particular $2p - 1s$ transition, if the excited Ne cascades according to the sequence $3s - 2p - 1s$, without having any collisions during cascading. At intermediate afterglow times, there is sufficient intensity in some $3s - 2p$ and $4d - 2p$ transitions that their line shapes can be studied, indicating the possibility of a cascading contribution to the $2p - 1s$ transitions. (Although the intensities of these lines from higher states are modest, rather large numbers of these and even higher states may be involved, since transitions from $6d_4$, $5s_5$, etc., all of which may cascade to $2p$, have been noted well into the afterglow, ~ 1 msec⁽⁶⁾).

As noted below, there is reason to assume that the molecular ions undergoing recombination are in different electronic and/or vibrational states. If this is true, different values of the kinetic energy of dissociation, E_D , are to be expected. Since the Doppler widths of the atomic light in the afterglow are determined by the E_D values, a superposition of several trapezoids having different E_D values will result⁽⁷⁾. Thus, the lineshape may look like

the schematic Fig. 3, having shoulder pairs α , β , $\Delta_{1,2,3}$, ... for every intersection of the repulsive excited state curves x_1 with the molecular ion curves i_1 in Fig. 1, with relative intensities given by overlap-survival factors. Hence, the actual lineshape can become very complex, particularly if an atomic level $2p_n$, with a large angular momentum, splits into many curves of the type x_1 , having many crossings with the ionic curves (or near-crossings of the type Δ). Indeed, we find evidence that some of the experimental lineshapes apparently are more of the type suggested by Fig. 3 than of the simple trapezoidal form first mentioned.

Since the atomic energy levels $U(2p_n)$ are precisely known⁽⁸⁾, and the E_D 's can often be measured from the widths of pairs of shoulders in the line profiles, energy levels U_x of several of the ionic states, where

$$U_x = U(2p_n) + E_D^x, \quad (5)$$

can sometimes be inferred from our measurements. (U_x is taken from the atomic ground state.) Among the line shapes studied, if two transitions originate from the same upper state $2p_n$, then equal U_x values are to be expected (see Fig. 1). In addition, analysis of radiative transitions with different upper states may lead to the inference of equal U_x values, if the excited molecule repulsive curves leading to these different atomic states cross the same molecular ion curve (for example, curves x_2 and y_2 in Fig. 1). On the other hand, if curves such as x_1 and y_2 are involved, different values of U_x will be inferred from studies of transitions originating from different upper states. These general considerations, which are discussed further in Sec. V, should be borne in mind when interpreting the results below.

IV. Experimental Results

A. Discharge line shapes in neon

The forms of the discharge line profiles are determined by the densities and temperatures of the electrons, ions and neutrals. The most significant factor is the thermal Doppler broadening (together with the instrumental broadening), although a Stark broadening influence of the plasma (density, $n_e \sim 10^{10} \text{ cm}^{-3}$) and of the neutrals (density, $n_0 \sim 3 - 7 \times 10^{16} \text{ cm}^{-3}$) can be seen. In some cases a high density of absorbing ls states affects the discharge line profiles, which effect can usually be avoided by reducing the discharge excitation. In any case, the line widths under discharge conditions could definitely be made smaller than those of all of our afterglow lines, whereas, without dissociative recombination, the afterglow lines would be expected to be of smaller half-width, because of the smaller plasma densities ($\lesssim 10^9 \text{ cm}^{-3}$) at the afterglow times of interest here.

Fig. 4 shows an example of the Neon $\lambda 5852$ and $\lambda 6678$ discharge lines. The computed thermal Doppler half-widths at 77°K are 20 mK and 18 mK, respectively; whereas the observed half-widths are 43 mK and 37 mK⁽⁹⁾. A part of the differences (between 20 and 43 mK at $\lambda 5852$) is due to the instrumental width (estimated not to exceed 10 mK), the remainder probably being due to Stark broadening by neutrals and plasma. At twice the neutral density, the observed half-width of $\lambda 5852$ at 77°K is slightly larger ($\lesssim 50$ mK), and at the same neutral density at 300°K and maximum available microwave discharge power, this half-width increases to ~ 70 mK, which clearly is an effect of both increased temperature and plasma density.

For all the other neon lines the situation is approximately the same; the recorded half-widths are generally about two times larger than their computed 77°K Doppler widths and can be affected by changing either the plasma or the neutral atom densities. Similarly, in Argon for $\lambda 6965$ and for $\lambda 7067$ at 77°K

the recorded half-widths are 29 mK and the computed Doppler half-widths are about 14 mK.

The small component of the line shifted 74 mK to the right in the $\lambda 5852$ profiles of Fig. 4 is due to the isotope Ne_{22} , which has a relative abundance of $\sim 9\%$ ⁽¹⁰⁾ compared to the main isotope Ne_{20} . In Argon no isotope lines can be seen.

B. Neon afterglow line intensities

In a neon afterglow, many fairly intense lines can be studied. All the strong $2p - 1s$ transitions, which are familiar from spectroscopic work on discharges, are present in the afterglow. Except possibly for the first few hundred microseconds of an afterglow, all these lines decay at the same rate, which indicates their equivalence for the purposes of our present study. Examples of the observed decays of four of the lines are shown in Fig. 5. The "intensities" shown here are simply the photomultiplier output currents and have not been corrected for the changing efficiency of the EMI 9558 photocathode with wavelength; however, the corrected relative intensities of all the lines are given in Table I, from which one may assess the relative strengths of the recombination radiations.

The rather complicated decay (approximately as $1/t$) shown in Fig. 5 evidently results from the fact that the recombination radiation intensity is proportional to the product $(\alpha_j M n_e)$, where α_j is the recombination coefficient into the radiating excited state, M is the molecular ion density and n_e the electron density. At low pressures, both atomic and molecular ions are present in the afterglow. In the discharge some molecular ions are produced from highly excited atoms by associative ionization, i.e.,



Table I. Atomic line profiles studied and their relative intensities (photon/sec) during the afterglow.

line $^{\circ}$ [A]	rel. intens.	transition (Paschen)	line $^{\circ}$ [A]	rel. intens.	transition (Paschen)
Ne 5852	1.0	$2p_1 - 1s_2$	Ne 6532	0.20	$2p_7 - 1s_3$
5400	<<1	- $1s_4$	6383	0.71	- $1s_4$
6598	0.57	$2p_2 - 1s_2$	6217	0.15	- $1s_5$
6163	0.40	- $1s_3$	7173	<<1	$2p_8 - 1s_2$
6029	0.15	- $1s_4$	6506	0.85	- $1s_4$
6074	0.47	$2p_3 - 1s_4$	6334	0.33	- $1s_5$
6678	1.11	$2p_4 - 1s_2$	6402	1.60	$2p_9 - 1s_5$
6096	0.67	- $1s_4$	7245	0.24	$2p_{10} - 1s_4$
5944	0.40	- $1s_5$	Ar 6965		$2p_2 - 1s_5$
6717	0.54	$2p_5 - 1s_2$	7383		$2p_3 - 1s_4$
6266	0.57	- $1s_3$	7067		$2p_3 - 1s_5$
6929	0.45	$2p_6 - 1s_2$	7948		$2p_4 - 1s_3$
6304	0.15	- $1s_4$	7635		$2p_6 - 1s_5$
6143	0.65	- $1s_5$			

while during the afterglow they are produced from atomic ions by the rather slow three body conversion reaction⁽¹¹⁾,



Thus, since M and n_e can have quite different time histories in low pressure afterglows, the excited state production by recombination and consequently the associated afterglow radiation can exhibit rather complicated decays.

In the three-body formation of Ne_2^+ (Eq. 7) the molecular ions may be formed in any vibrational and electronic state. Since the molecular ion "lifetime" before recombination with an electron varies between $\sim 100 \mu\text{sec}$ and $\sim 5 \text{ msec}$, depending on the electron density, relaxation of the vibrational state populations to a thermal distribution may not always take place during the afterglow. Thus, as noted in the previous section, additional contributions to the line profiles would occur as a result of the " Δ -crossings" between the vibrationally excited ion states and the repulsive neutral states (see Figs. 1 and 3).

C. Neon afterglow line profiles

Recordings of most afterglow line profiles could be taken at any afterglow time between 0 and $\sim 10 \text{ msec}$, i.e. at electron densities between $\sim 10^{10}$ and $\sim 10^8 \text{ cm}^{-3}$. With the possible exception of the first few hundred microseconds, there is no noticeable variation of recorded lineshape with time, and Fig. 6 is typical of the $\lambda 5852$ line shape for the whole accessible afterglow interval between 0.5 and 10 msec. Also, a gas temperature variation from 300 to 77 °K hardly affects the afterglow line shape, whereas discharge line shapes are definitely reduced in width at the lower temperature. (For a recording of the $\lambda 5852$ line shape taken at 300°K see Figs. 9 and 10 of the paper

by Connor and Biondi⁽¹⁾).

A careful examination of line profile tracings (as many as 13 interference orders are usually traced for a given set of afterglow conditions) reveals that the $\lambda 5852$ structure is more complicated than the single trapezoidal shape given by Eq. (2) on which is superposed a thermal doppler core (see, for example, the residual "shoulders" at frequency shifts greater than 150 mK from line center, as indicated by the letters b - b in Fig. 6). It is a straightforward matter to show that two "shoulders" corresponding to two different dissociation energies E_D' and E_D'' , yield a discernable "step" between them only if

$$\left(E_D'^{1/2} - E_D''^{1/2} \right) > 2(kT)^{1/2}. \quad (8)$$

At dissociation energies of ~ 1 eV at $T = 77^\circ\text{K}$, an energy difference in excess of ~ 0.3 eV is required; thus, not all of the structure corresponding to different initial states in the dissociative recombination reaction can be detected in the line profiles, especially when one considers the additional effects of instrumental broadening of the profile and the inevitable "noise" in an afterglow trace (see, for example the slight irregularity in the tracing near the line center in Fig. 6).

In analyzing the profiles of the various afterglow lines, we have adopted the procedure of examining many different tracings of a given line and selecting only those shoulder pairs which are symmetrically disposed with respect to the line center, and of nearly equal amplitude. Thus, although a single tracing is sufficiently "noisy" to render doubtful the reality of some of the shoulder steps, the reproducibility of the position of the steps on many tracings gives us some confidence in the existence of substantial structure in the line profiles.

Let us now consider some of the line profiles in detail, starting with

the afterglow $\lambda 5852$ ($2p_1 - 1s_2$) line of Fig. 6. The apparent slight asymmetry in the shoulder structures indicated by the positions of the horizontal lines in Fig. 6 stems from the neon isotope Ne_{22} , which is present with its natural abundance of about 9%. (No attempt has been made to use a gas sample with enriched Ne_{20} .) A simple quantitative decomposition of the observed profile into a Ne_{20} and a Ne_{22} line, with relative intensities of 91:9, the latter shifted by 74 mK to the right, reveals perfectly symmetric shoulder intensities for the main isotope. A good approximation of this symmetric structure can be obtained by using the left wing of the profile only, complementing it on the right of the line center by its mirror image. In the discussions to follow, the Ne_{22} isotope will not be considered further.

An interesting feature of the $\lambda 5852$ afterglow profile is that it can very nearly be understood as a superposition of one dissociative trapezoid (C - C in Fig. 6) and a narrow thermal core, as was pointed out by Connor and Biondi⁽¹⁾. Under this assumption, the kinetic energy of dissociation, E_D , can be evaluated from the apparent half-width (280 mK), yielding $E_D = (1.25 \pm 0.07)$ eV. Hence the energy of the molecular level with regard to the atomic ground state would be $U_x = (20.21 \pm 0.07)$ eV and the molecular ion binding energy $D = (1.35 \pm 0.07)$ eV, in close agreement with the results of the earlier paper⁽¹⁾. (In deriving this value of the dissociation energy D , the ion is assumed to be in its ground vibrational and electronic states, which assumption may be called into question by the results of the present study).

A careful evaluation of our more accurate $\lambda 5852A$ afterglow line profiles indicates the presence of more features in the wings of the line than predicted by the simple theoretical shape of Eq. (2). In addition to the (trivial) isotope modification, a $\sim 50\%$ increase in length of the rise of the outermost prominent shoulders (C - C) is observed. It is just possible that this prolonged rise is largely instrumental or is due to gas temperatures substantially higher

than 77°K. It is also possible that momentum transfer collisions have affected the shape of the profile⁽¹⁾. We believe, however, in an alternative interpretation, that the deviations are the result of a more complex line structure having several shoulder pairs, similar to the case illustrated schematically in Fig. 3, with barely resolved step structures.

Favoring this interpretation is some just discernible structure, at the positions indicated by the lower case letters in Fig. 6. Each of the marked shoulder pairs is perfectly symmetric with regard to the line center, is reproducible through many orders (except for occasional interference by noise) and has essentially the predicted rise length, and the corresponding right and left shoulders are of equal amplitude (after correction for Ne_{22}). Furthermore, as will be shown below, other neon afterglow lines indicate similar structures. Hence we conclude that the $\lambda 5852$ line has a complex, multi-shoulder structure.

The line profiles of the remaining strong $2p - 1s$ transitions in neon are all of the multi-shoulder type. There are a number of lines which, similar to the $\lambda 5852$ line, could possibly be interpreted as a superposition of but one dissociative trapezoid and a narrow thermal core. Fig. 7, which shows the $\lambda 6598$ ($2p_2 - 1s_2$) afterglow profile, is another example of this type. However, a close inspection of many tracings of $\lambda 6598$ profiles indicates a more complex structure with several shoulder pairs at the positions indicated in Fig. 7. An example of an afterglow line profile which can hardly be understood as a superposition of a single dissociative trapezoid plus a thermal core is $\lambda 6304$ ($2p_6 - 1s_4$), as shown in Fig. 8. Comparison with the thermal discharge profile again suggests the presence of a number of shoulder pairs, only one of which (D - D) is apparent on a single trace, as indicated by the letters in the figure. There is also one particular line, $\lambda 6402$ ($2p_9 + 1s_5$), see Fig. 9, in which deviations from the thermal doppler profile yield a relatively narrow dissociative base, suggesting small E_D values. If we accept

this value, a substantially greater "binding energy" for the molecular ion of ~ 2.4 eV is derived (in disagreement with the value quoted earlier from previous $\lambda 5852$ studies), and a molecular ion curve of the type i_3 in Fig. 1 is implied. A detailed discussion of this point is deferred to Sec. V.

D. Argon line profiles

In argon similar line profiles have also been found. The discharge lines are approximately of the expected widths (thermal Doppler width and instrumental width) and all afterglow lines studied definitely have broader bases. As an example, Fig. 10 shows the measured $\lambda 6965$ ($2p_2 - 1s_5$) line profiles in Argon. In addition to this line, four other $2p - 1s$ transitions have been studied; $\lambda 7067$, $\lambda 7383$, $\lambda 7635$, and $\lambda 7948$.

There is some evidence that the afterglow line profiles have multishoulder structures similar to those in neon. The structures are narrower and thus less readily resolved, however. We therefore have refrained from attempting to derive E_D values from the argon profiles because of the large errors associated with such attempts. We do, however, conclude that the only likely source of such broadened afterglow line profiles is the dissociation kinetic energy given to the excited argon atom formed during recombination, giving evidence of the connection of the large electron capture rate in argon with the dissociative recombination process.

V. Discussion

The conclusions of the present study may be summarized as follows:

1. The 22 neon and 5 argon [$2p_n \rightarrow 1s_m$] transitions studied (see Table I) all reveal afterglow line profiles which are broader than the corresponding discharge lines. In addition, in most cases the forms of these afterglow profiles are clearly consistent with dissociation kinetic energy contributions to the broadening. Thus, we are led to the conclusion that, in neon, all of the excited atomic states $2p_n$ ($1 \leq n \leq 10$) are products of the dissociative

recombination process. In addition, preliminary line shape studies suggest that even higher levels, such as 3s and 4d, are formed during dissociative recombination of electrons and Ne_2^+ ions. In argon, while the afterglow line shapes are not as well defined, their obvious broadening relative to the discharge lines indicates that here, also, $2p_n$ excited states are formed during dissociative recombination of electrons with Ar_2^+ ions.

2. Examination of the line profiles (at the improved signal-to-noise ratios obtained in the present studies) reveals that the afterglow line shapes are more complicated than a single dissociative pedestal (of the form given by Eq. 2) surmounted by a thermal core. The lines are evidently multi-shouldered in structure, and comparisons of tracings of a given profile through many successive interference orders reveal the positions of not only the strong shoulders (such as C - C in Fig. 6) but also weaker features (such as a - a and b - b in Fig. 6).

3. From the inferred values of the dissociation kinetic energies for these various shoulders, together with Eq. (5), one can calculate the initial molecular ion levels from which the dissociative process started. Examples of the energy level values inferred from the five $2p_1$ and $2p_2 \rightarrow 1s_m$ atomic transitions studied are contained in Table II. The accuracy of the inferred values varies considerably in going from "strong" to "weak" features in a line profile (from ~ 0.01 eV to $\gtrsim 0.1$ eV), but it will be seen that there do seem to be intervals of a few tenths of an eV between levels. (This interval is approximately that given by the "discernible step" resolving criterion of Eq. 8.) In addition, as noted in Sec. III, not only do two different lines from a common upper state appear to reproduce the molecular ion levels within ~ 0.1 eV, but also lines from different upper states, i.e. $2p_1$ and $2p_2$, yield consistent molecular ion levels, suggesting that although the analysis is relatively crude and incomplete it does provide some information concerning

the energy levels. (An apparent inconsistency in the observed profiles is that the strong shoulders C - C of $\lambda 5852$ in Fig. 6, which yield the molecular level at 20.22 eV, appear as a weak feature in $\lambda 5400$, which originates from the same upper state; however $\lambda 5400$ is a very weak afterglow line, leading to difficulties in the shoulder position determinations.)

4. From a consideration of the positions of the inferred molecular ion energy levels and the strengths of the corresponding features in the line profiles, it is clear that the actual potential curves involved in the dissociative recombination of electrons and Ne_2^+ ions are much more complicated than the schematic representation given in Fig 1 of Connor and Biondi's paper⁽¹⁾. Although we arrive at a similar pair of curves (i_2 and x_2 in our Fig. 1), the additional higher energy structure in the $\lambda 5852$ profile, together with that from other spectral lines studied, leads us to postulate an additional bound Ne_2^+ state of the form of curve i_1 which is reached by the unstable excited molecule curve x_1 with crossings α and β' of the ion curves.

A final point concerning the Ne_2^+ energy levels is the question of the reality of the curve labelled i_3 in Fig. 1. Although there are substantial numbers of just discernible, narrow shoulders near the thermal cores of most of the lines, leading to the inference of molecular ion energy levels at less than 20 eV above the atomic ground state, we noted in Sec. III that cascading from higher states could also lead to such narrow shoulders. Arguing against a Ne_2^+ state with ~ 2.7 eV binding energy (curve i_3) is the fact that the threshold for associative ionization (reaction 7) has been determined⁽¹²⁾ to be 20.86 ± 0.20 eV above the atomic ground state, which is consistent with a flat or slightly attractive excited molecule curve crossing our i_2 curve, whose minimum is at ~ 20.2 eV. (Strongly attractive, i.e. bound state Ne_2^* , curves seem unlikely inasmuch as band spectra of neon molecules have not been observed.) Thus, associative ionization does not require a deeper bound state of Ne_2^+ .

Table II. Molecular ion energy levels calculated from the dissociation kinetic energies, E_D^x , of the atoms produced by dissociative recombination. The E_D^x values are obtained from the multi-shouldered structure in the line profiles. Parentheses around a value indicate that it is less certain, while an asterisk indicates the presence of a very weak feature in the line structure.

while an asterisk indicates the presence of a very weak feature in the line structure.																
Neon Line [Å]	Transition (Paschen)	$U(2p_n)$ [eV]	Molecular ion level, $U_x = U(2p_n) + E_D^x$, [eV]													
5852	$2p_1 - 1s_2$	18.92	21.2	*	-	20.7	(20.4)	20.2	(20.1)	19.8	(19.7)	19.4	-	19.1	*	-
5400	- $1s_4$		(21.2)	(21.1)	-	(20.8)	(20.4)	-	(20.1)	(20.0)	(19.8)	(19.3)	-	(19.2)	*	-
6598	$2p_2 - 1s_2$	18.69	21.1	-	21.0	20.7	-	20.3	20.0	-	19.7	19.5	19.3	19.2	-	19.0
6163	- $1s_3$		21.2	-	-	*	-	20.3	*	-	19.7	19.5	-	*	-	*
6029	- $1s_4$		21.2	-	-	20.7	20.4	20.2	20.0	-	-	19.5	-	19.2	19.1	19.0

In addition, the ~ 2.7 eV binding energy of i_3 is about twice the estimated value from chemical bond considerations⁽¹³⁾ and is also much higher than the binding energy derived from scattering data⁽¹⁴⁾.

We, therefore, conclude that there probably is no i_3 -type bound state for Ne_2^+ and that the narrow shoulders on the $(2p_n \rightarrow 1s_m)$ line profiles are the result of recombination into higher ($\geq 3s, 4d$) states, followed by radiative transitions into $2p_n$ states before loss of the small dissociation kinetic energy acquired in the initial recombination event. In support of this are some preliminary studies of higher state line profiles in the earlier afterglow (0.6 - 1.5 msec), for example, the $\lambda 5689$ ($3s_5 \rightarrow 2p_{10}$) transition. This line appears to be multi-shouldered, and E_D values of 0.20 and 0.38 eV are inferred. Since corresponding E_D values have been noted for some of the $(2p_n \rightarrow 1s_m)$ transitions, a cascading origin of the small dissociation energies in these latter profiles seems reasonable.

VI. Acknowledgements

The authors are indebted to R. Hake for his assistance in obtaining some of the data presented in this paper. One of us (L. F.) acknowledges, with thanks, helpful discussions with W. W. Robertson and the support of the Joint Services Electronics Program (research grant AF-AFOSR-766-67) during the preparation of the paper.

References

1. T. R. Connor and M. A. Biondi, Phys. Rev. 140 A778 (1965).
2. W. A. Rogers and M. A. Biondi, Phys. Rev. 134 A1215 (1964).
3. Paschen notation is used to designate the neon and argon states. Subscripts are omitted wherever there is no need to be specific.
4. G. Farkas and P. Varga, J. Sci. Instr. 41 704 (1964).
5. L. Frommhold and W. A. Feibelman, J. Sci. Instr. 44 182 (1967).
6. At the "low" electron densities of the present studies ($\lesssim 10^{10} \text{ cm}^{-3}$) population of excited states by collisional-radiative recombination should proceed at a small rate compared to the dissociative recombination process.
7. Unfortunately, if the 2p levels are also populated by cascading from a sequence of higher states (e.g. 4d, 5d, 6d ...) formed by recombination, one would also see sets of narrow shoulder pairs.
8. C. Moore, Atomic Energy Levels, Vol. I. Circ. 467, (Nat. Bureau of Standards, Washington, D. C., 1949).
9. The wave number unit is the Kayser; $1 \text{ cm}^{-1} \equiv 1\text{K}$.
10. R. Ritschl and H. Schober, Phys. Zeitschrift 38 6 (1937).
11. G. F. Sauter, R. A. Gerber, and H. J. Oskam, Physica 32 1921 (1966).
12. M. S. B. Munson, J. L. Franklin, and F. H. Field, J. Phys. Chem. 67 1542 (1963).
13. L. Pauling, The Nature of the Chemical Bond, (Cornell Univ. Press, Ithaca, N. Y., 1960) p. 356.
14. E. A. Mason and J. T. Vanderslice, J. Chem. Phys. 30 599 (1959).

Figure Captions

Fig. 1. Schematic representation of the potential energy curves of the Ne_2^+ ion and some of the repulsive excited molecule curves leading to the $2p_n$ excited atomic states. The shapes of the curves are not meant to be significant; only the energy levels of the Ne_2^+ states and the curve crossings are semi-quantitative.

Fig. 2. Simplified diagram of the microwave afterglow/optical interferometer apparatus used in the line shape studies.

Fig. 3. Hypothetical line shape arising from superposition of several dissociation kinetic energies and a thermal doppler core. The contributions, α , β , γ , Δ_1 , might arise from energy states and curve crossings of the type indicated by the corresponding letters in Fig. 1.

Fig. 4. Chart record of neon line profiles during the microwave discharge at $T = 77^\circ\text{K}$ and $p_0 = 1$ Torr (reduced to 0°C); (a) $\lambda 5852$ ($2p_1 \rightarrow 1s_2$) and (b) $\lambda 6678$ ($2p_4 \rightarrow 1s_2$). The Ne_{20} and Ne_{22} isotope contributions are clearly resolved.

Fig. 5. Decay of intensity of several ($2p_n \rightarrow 1s_m$) neon transitions during the afterglow.

Fig. 6. Top: Chart record of the $\lambda 5852$ ($2p_1 \rightarrow 1s_2$) neon line profile taken during the period 0.6 - 1.0 msec of the afterglow. Bottom: Tracing of record showing positions of six pairs of "dissociative shoulders" with corresponding E_D values in eV of: a, 2.28; b, 1.73; c, 1.26; d, 0.88; e, 0.47; and f, 0.16. The thermal "core" of the line has a half width of ~ 31 mK.

Fig. 7. Chart record of the $\lambda 6598$ ($2p_2 \rightarrow 1s_2$) neon line profile taken during the interval 0.3 - 0.9 msec of the afterglow. The inferred positions of several of the shoulder pairs are shown by the horizontal lines.

Fig. 8. Tracing of the chart records of $\lambda 6304$ ($2p_6 \rightarrow 1s_4$) neon line profiles taken during the discharge and during the interval 0.6 - 1.2 msec of the afterglow. The inferred positions of the dissociative shoulders are indicated by

the letters.

Fig. 9. Chart record of the $\lambda 6402$ ($2p_9 \rightarrow 1s_5$) neon line profile taken during the interval 0.5 - 1.5 msec of the afterglow.

Fig. 10. Tracing (discharge line) and chart record (afterglow line) of $\lambda 6965$ ($2p_2 \rightarrow 1s_5$) argon line profiles. (The afterglow line was recorded during the interval 1.0 - 2.2 msec).

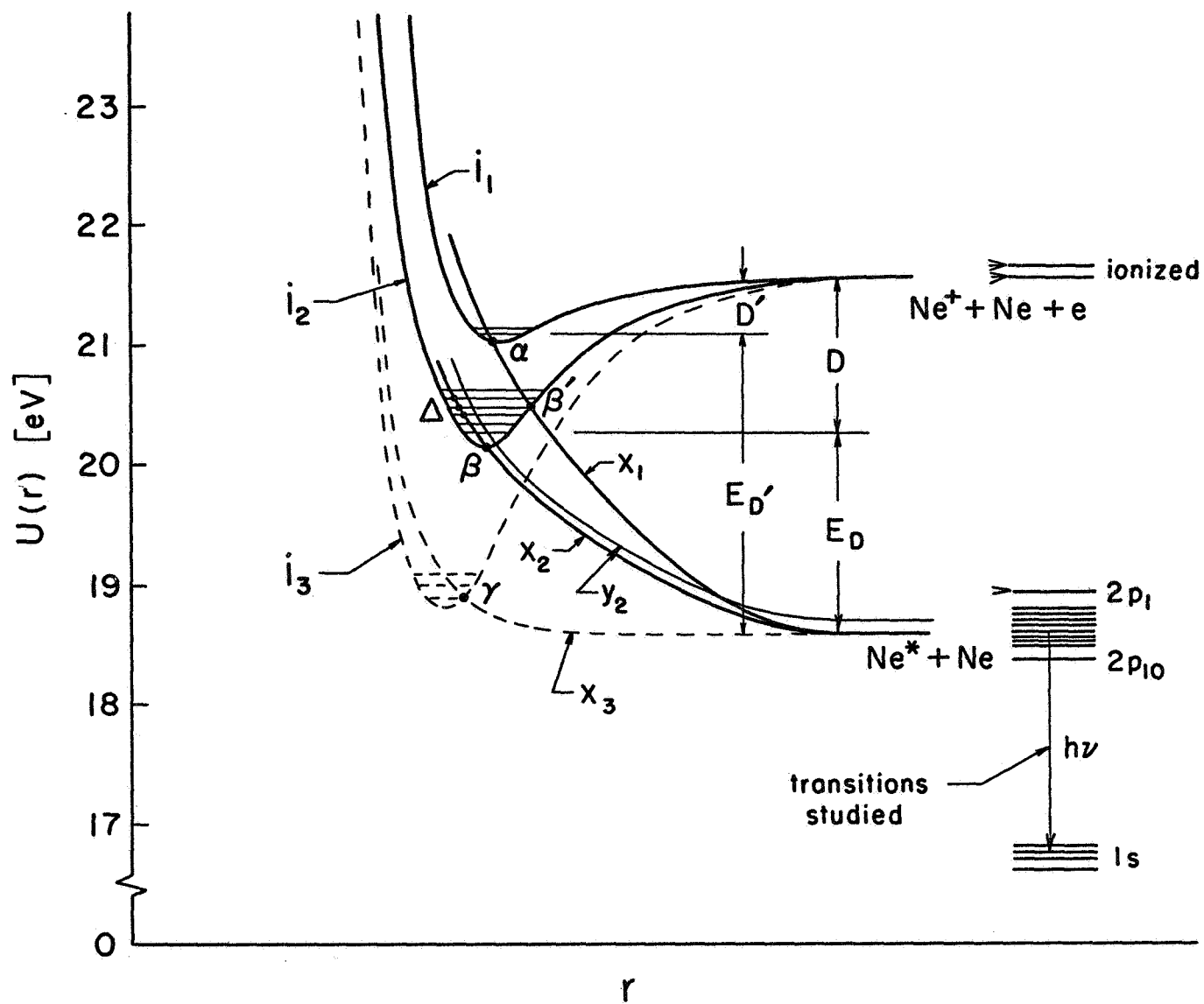


Figure 1

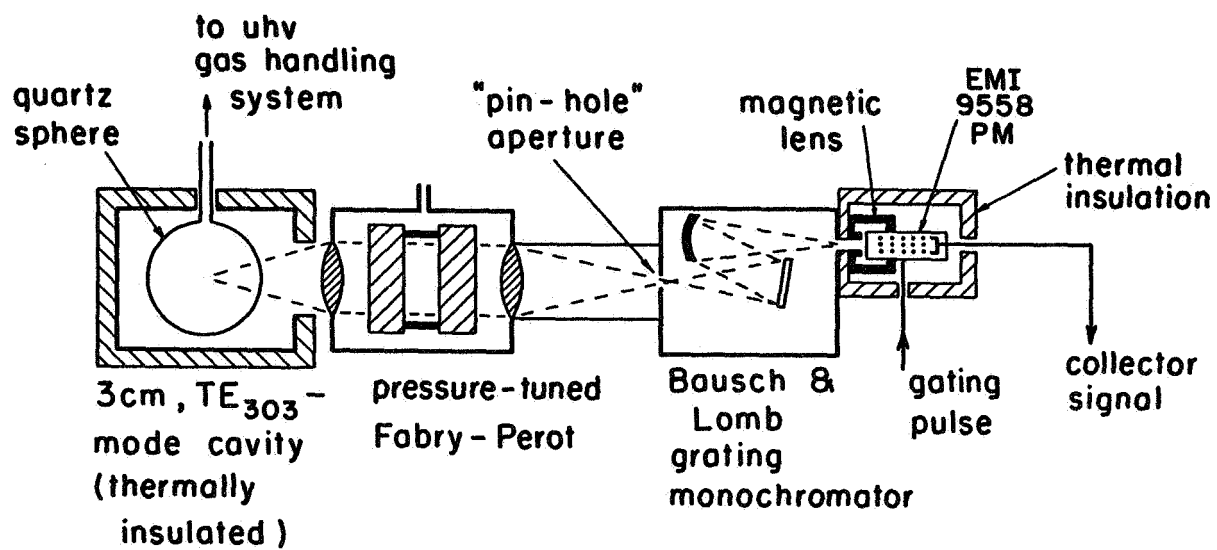


Figure 2

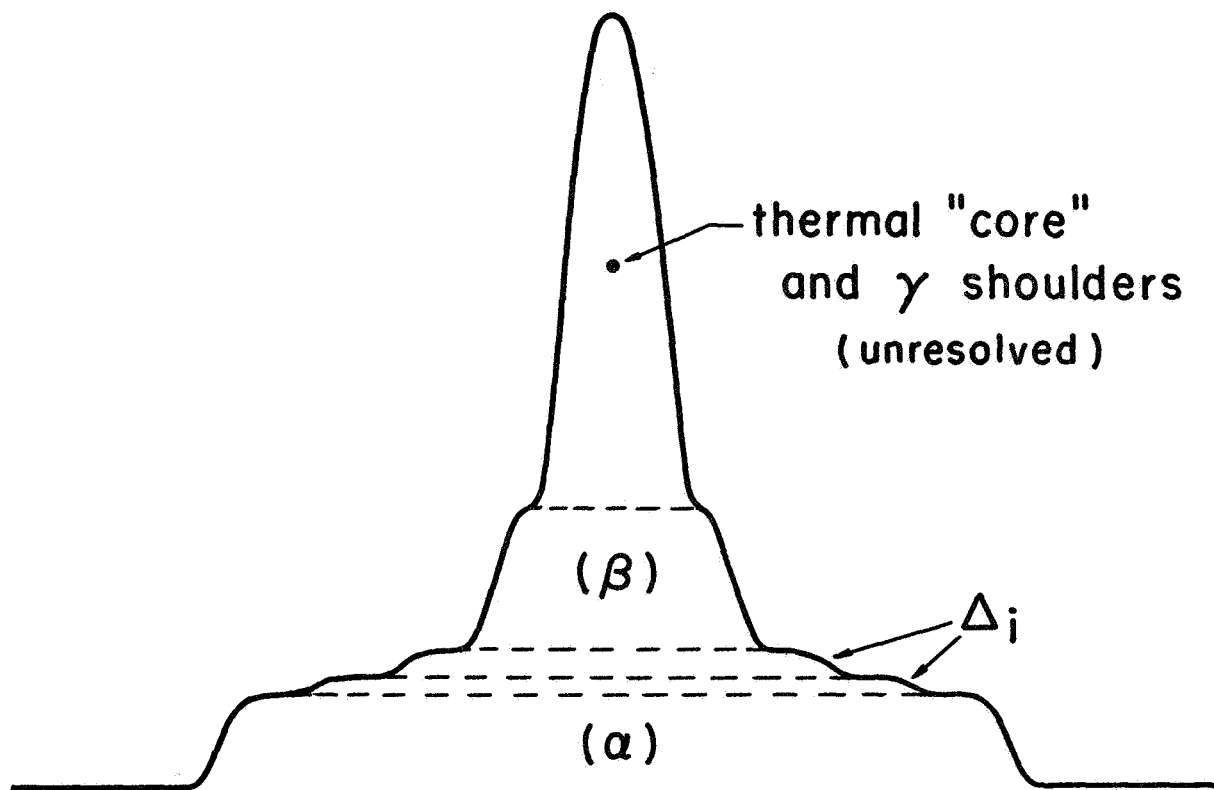


Figure 3

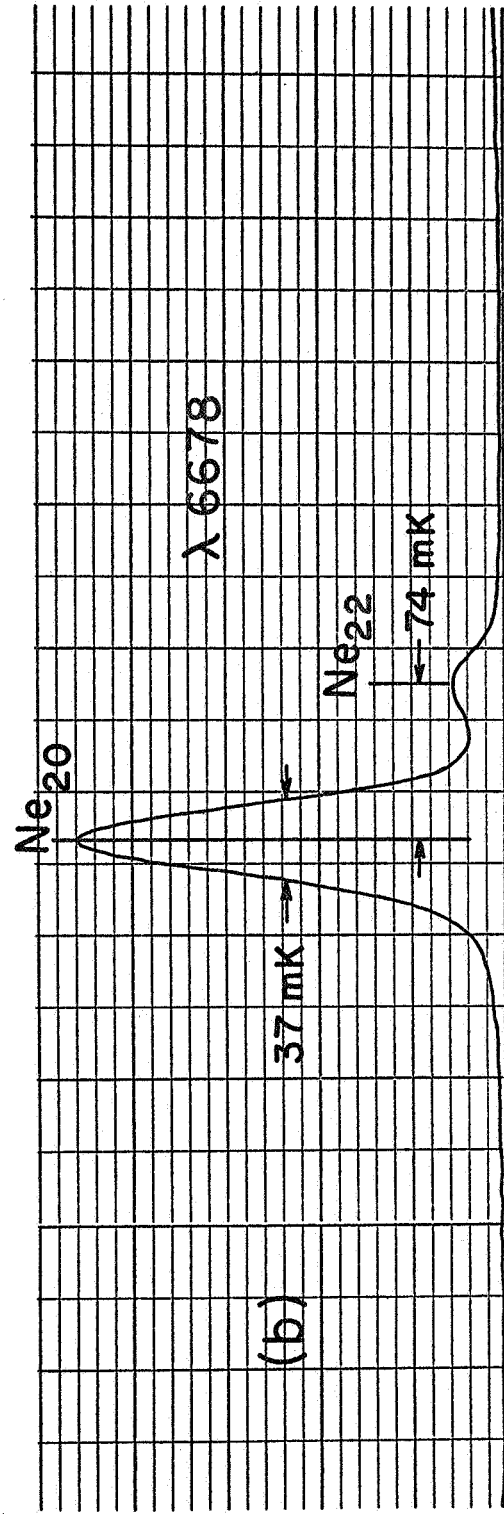
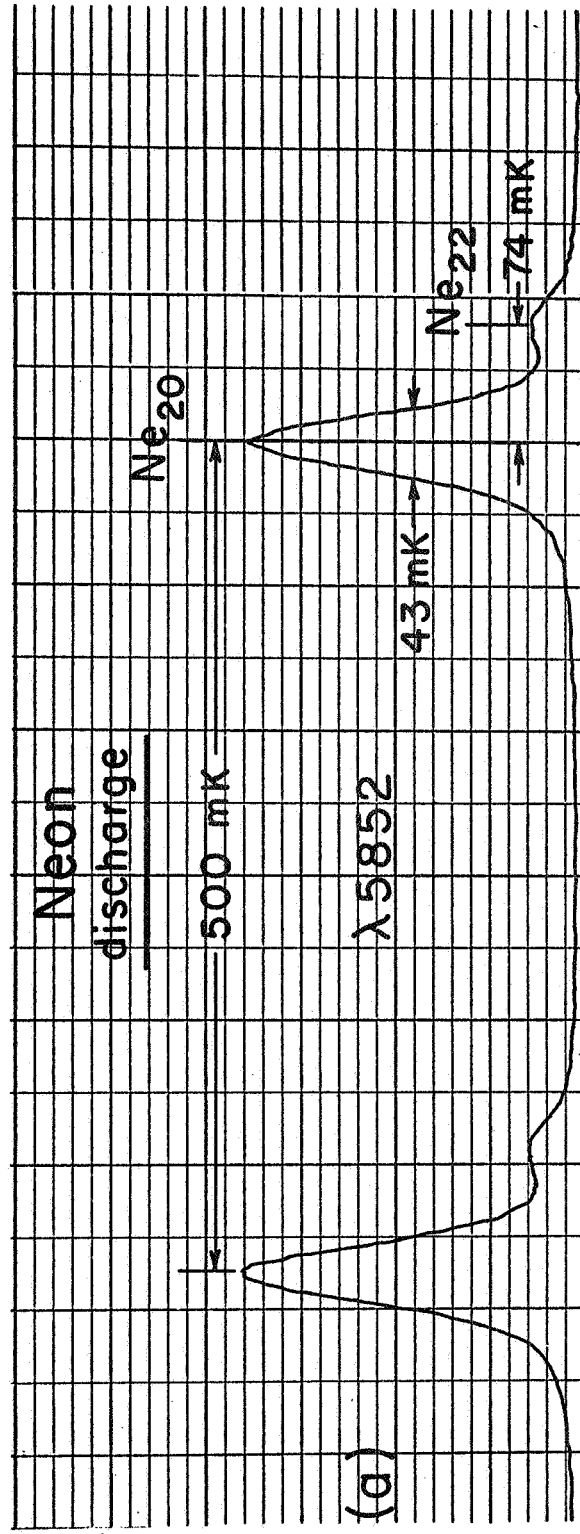


Figure 4

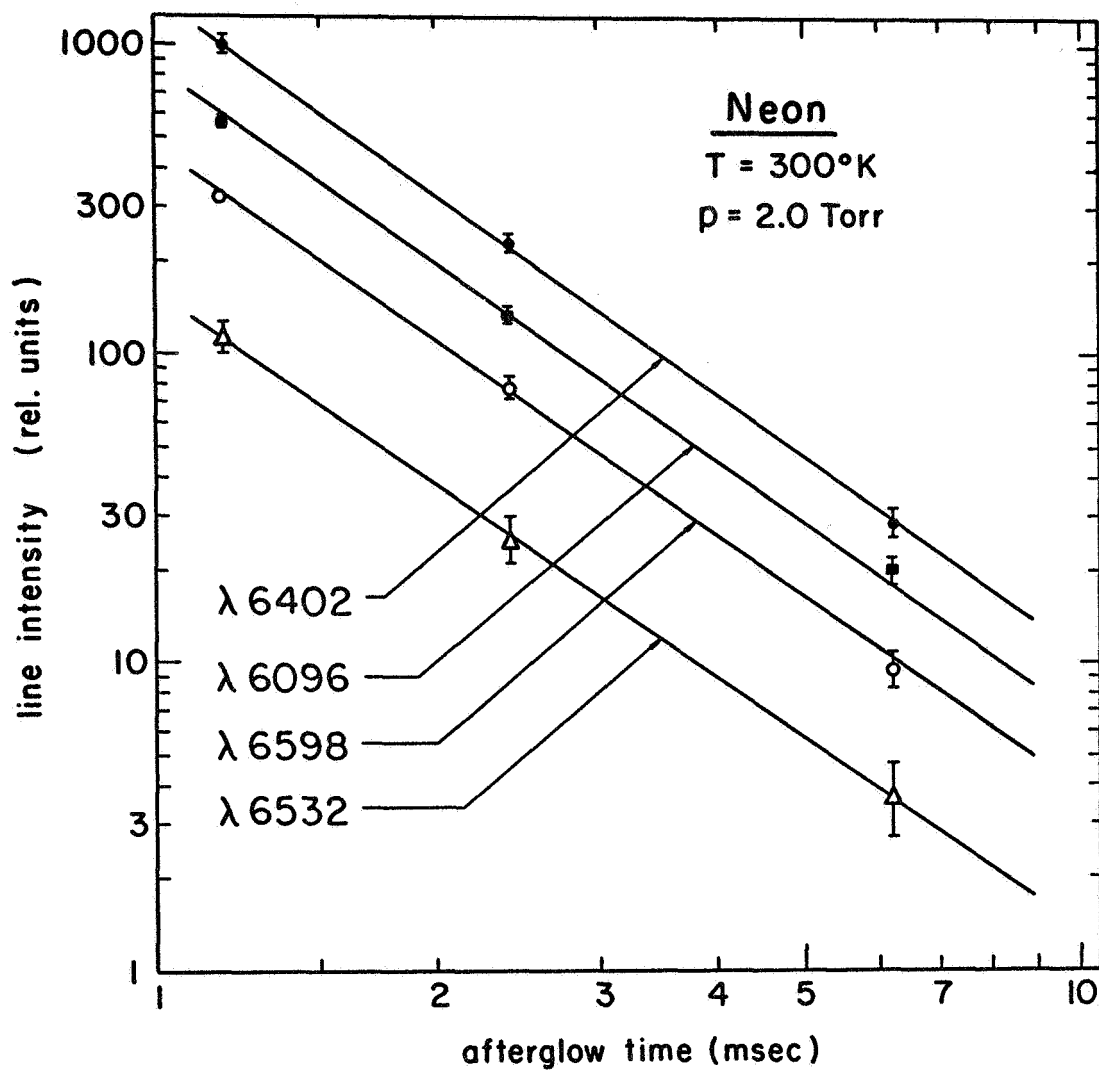


Figure 5

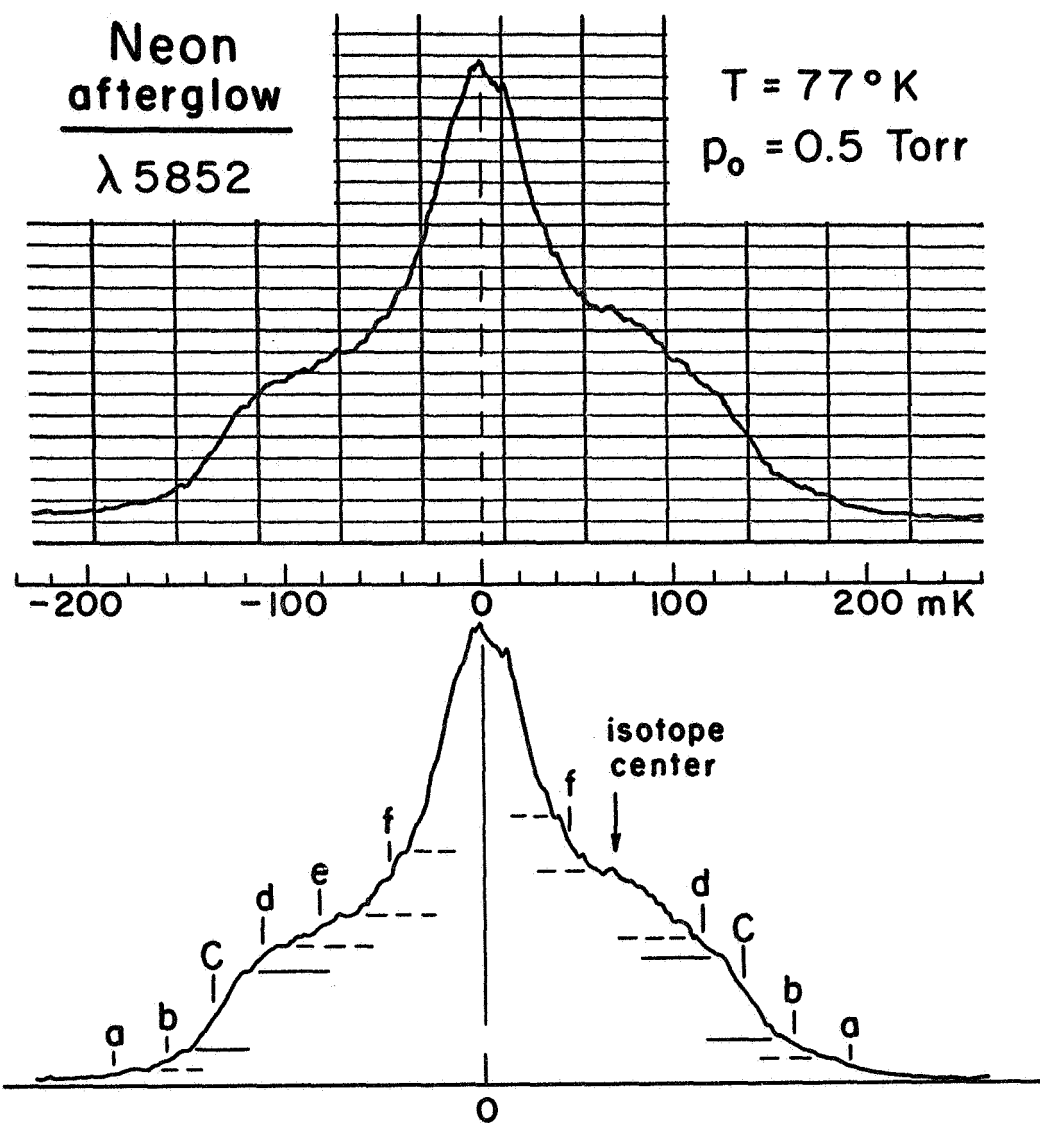


Figure 6

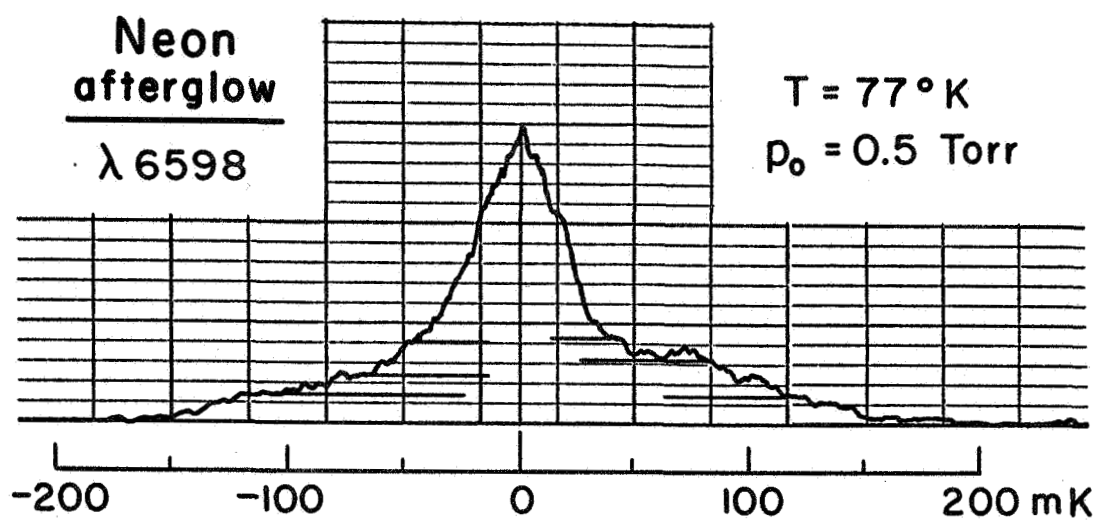


Figure 7

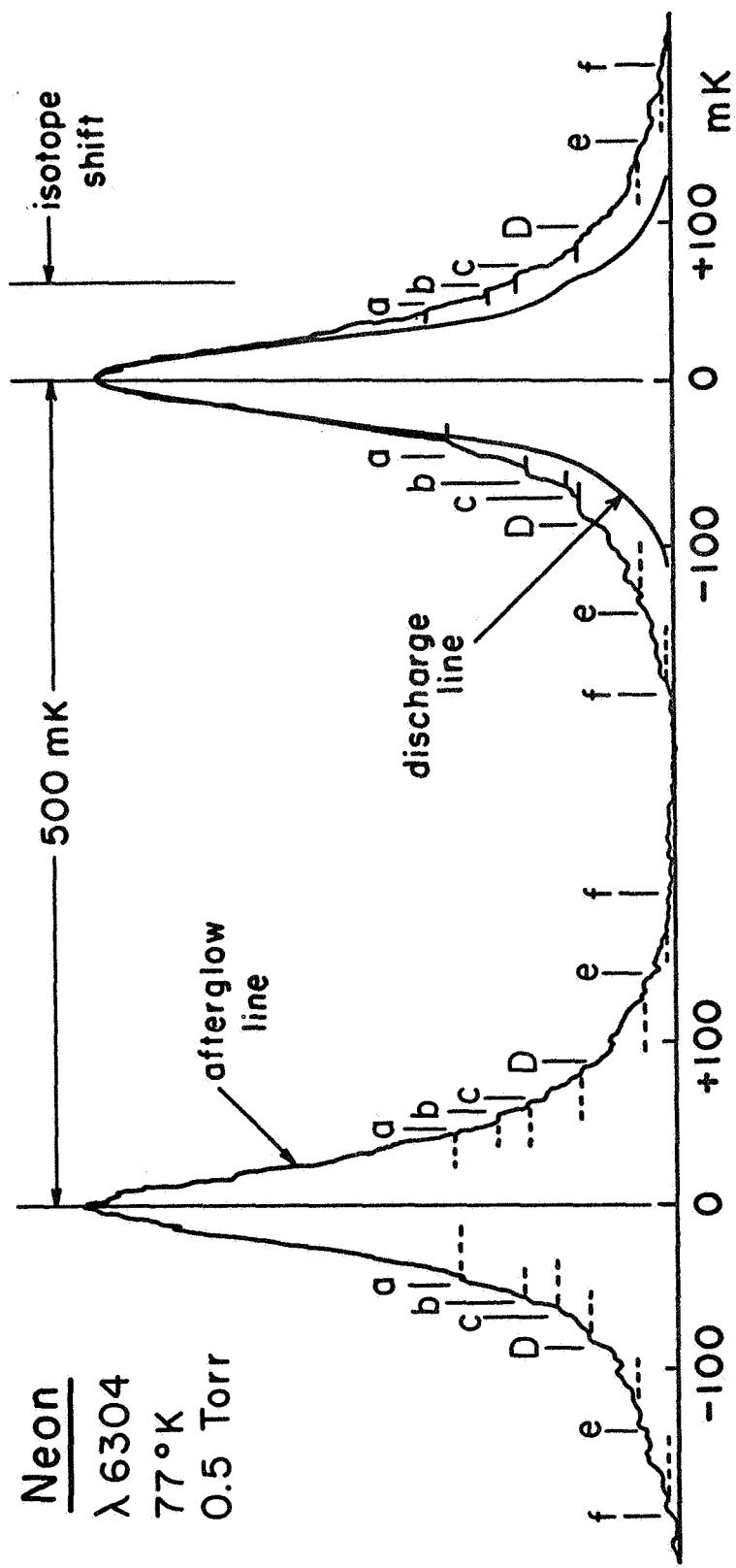


Figure 8

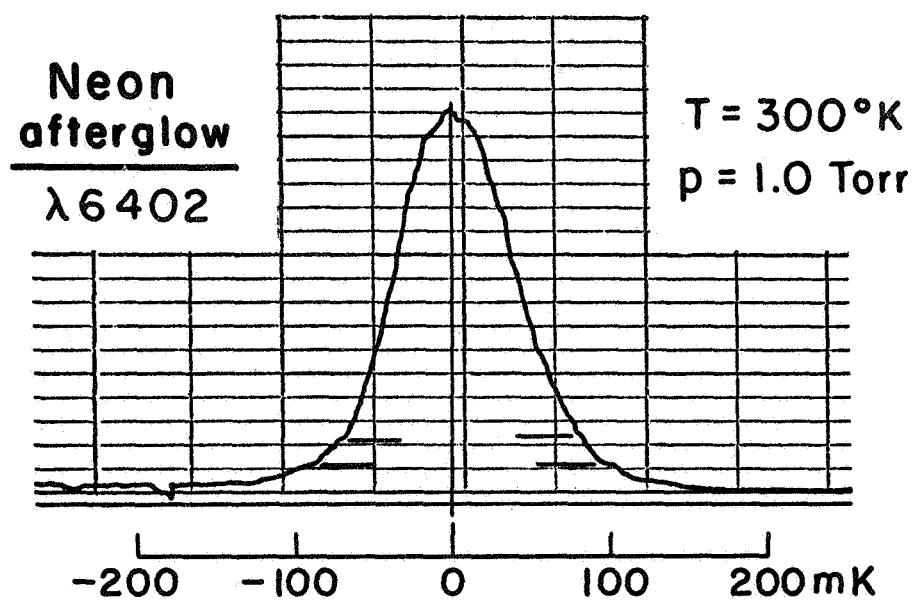


Figure 9

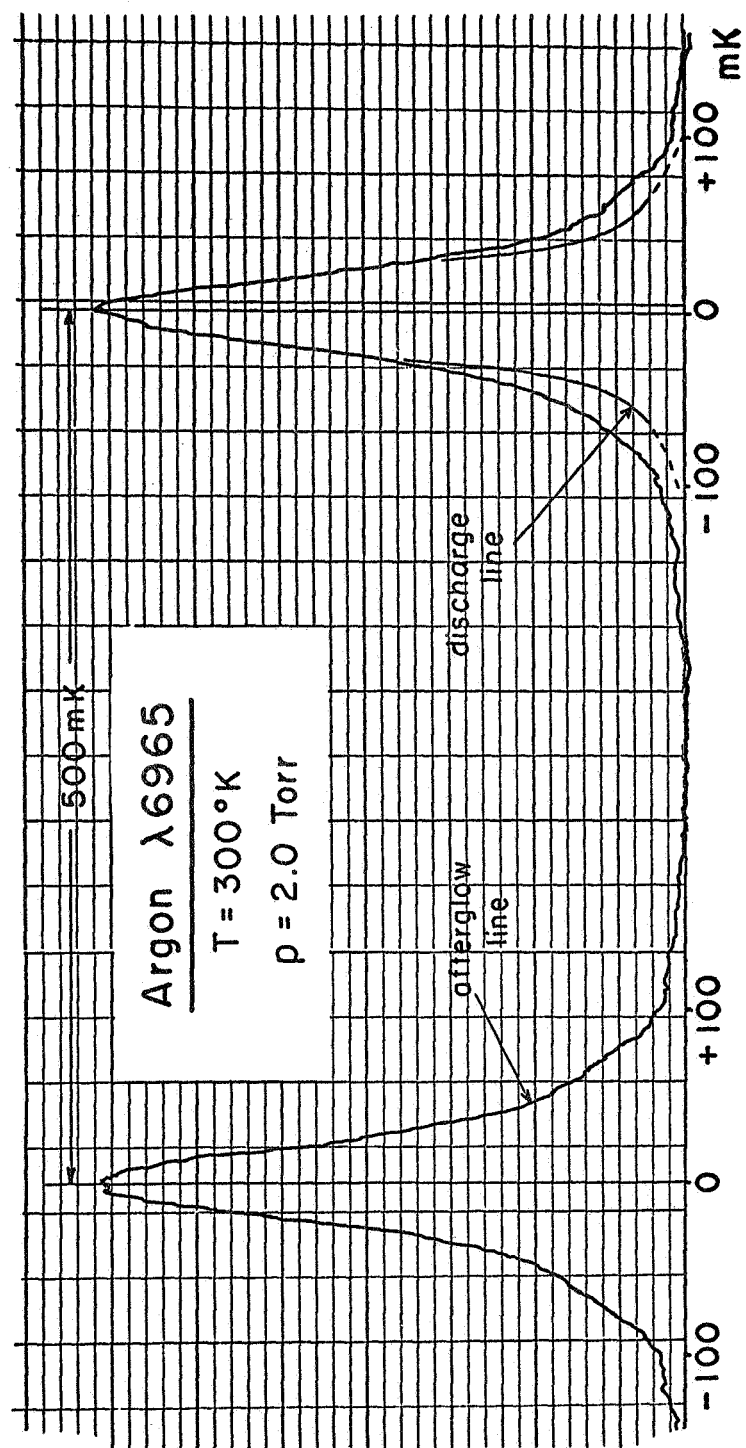


Figure 10